HHS Public Access

Author manuscript

J Biol Chem. Author manuscript; available in PMC 2015 July 27.

Published in final edited form as:

J Biol Chem. 2006 December 1; 281(48): 36977–36984. doi:10.1074/jbc.M607164200.

A Membrane-proximal Tetracysteine Motif Contributes to Assembly of CD3$\delta\varepsilon$ and CD3$\gamma\varepsilon$ Dimers with the T Cell Receptor*

Chenqi Xu[‡,1], **Matthew E. Call**[‡,§], and **Kai W. Wucherpfennig**[‡,§,¶,2]

[‡]Department of Cancer Immunology and AIDS, Dana-Farber Cancer Institute, Harvard Medical School, Boston, Massachusetts 02115

[§]Program in Immunology, Harvard Medical School, Boston, Massachusetts 02115

[¶]Department of Neurology, Harvard Medical School, Boston, Massachusetts 02115

Abstract

Assembly of the T cell receptor (TCR) with its dimeric signaling modules, CD3$\delta\varepsilon$, CD3$\gamma\varepsilon$, and $\zeta\zeta$, is organized by transmembrane (TM) interactions. Each of the three assembly steps requires formation of a three-helix interface involving one particular basic TCR TM residue and two acidic TM residues of the respective signaling dimer. The extracellular domains of CD3$\delta\varepsilon$ and CD3$\gamma\varepsilon$ contribute to assembly, but TCR interaction sites on CD3 dimers have not been defined. The structures of the extra-cellular domains of CD3$\delta\varepsilon$ and CD3$\gamma\varepsilon$ demonstrated parallel β-strands ending at the first cysteine in the C*XX*C*X*E*XXX* motif present in the stalk segment of each CD3 chain. Mutation of the membrane-proximal cysteines impaired assembly of either CD3 dimer with TCR, and little complex was isolated when all four membrane-proximal cysteines were mutated to alanine. These mutations had, however, no discernable effect on CD3$\delta\varepsilon$ or CD3$\gamma\varepsilon$ dimerization. CD3$\delta\varepsilon$ assembled with a TCRα mutant that lacked both immunoglobulin domains, but shortening of the TCRα connecting peptide reduced assembly, consistent with membrane-proximal TCRα-CD3$\delta\varepsilon$ interactions. Chelation of divalent cations did not affect assembly, indicating that coordination of a cation by the tetracysteine motif was not required. The membrane-proximal cysteines were within close proximity but only formed covalent CD3 dimers when one cys-teine was mutated. The four cysteines may thus form two intra-chain disulfide bonds integral to the secondary structure of CD3 stalk regions. The three-chain interaction theme first established for the TM domains thus extends into the membrane-proximal domains of TCRα-CD3$\delta\varepsilon$ and TCRβ-CD3$\gamma\varepsilon$.

The T cell receptor (TCR)[3] controls T cell development and function and is assembled from six distinct component polypeptides into an eight-chain complex. The TCR heterodimer is responsible for ligand recognition but lacks cytoplasmic signaling domains. Instead, it

*This work was supported by National Institutes of Health Grant RO1 AI054520 (to K. W. W.).

[2]To whom correspondence should be addressed: Tel.: 617-632-3086; Fax: 617-632-2662; Kai_Wucherpfennig@dfci.harvard.edu.

[1]Supported by a postdoctoral fellowship from the Arthritis Foundation.

[3]The abbreviations used are: TCR, T cell receptor; TM, transmembrane; SBP, streptavidin-binding peptide; PC, Protein C-derived peptide; HA, hemag-glutinin peptide; IP, immunoprecipitation; snIP, sequential nondenaturing immunoprecipitation; TBS, Tris-buffered saline; ER, endoplasmic reticulum; WT, wild type; mAb, monoclonal antibody; BisTris, 2-[bis(2-hydroxye-thyl)amino]-2-(hydroxymethyl)propane-1,3-diol.

associates through non-covalent interactions with three dimeric signaling modules, CD3$\delta\varepsilon$, CD3$\gamma\varepsilon$, and $\zeta\zeta$ (1–11). The ζ chain only has a short nine-amino acid extracellular domain and forms covalent dimers through a cysteine at position 2 of the predicted trans-membrane (TM) domain (3, 12, 13). The CD3γ, -δ, and -ε chains have more substantial extracellular components, and their Ig domains form noncovalent heterodimers through parallel β-strands, which create a β-sheet along the dimer interface. In each CD3 chain, a nine-amino acid segment with a highly conserved C*XX*C*X*E*XXX* motif connects this β-strand to the TM domain (1, 14–18).

Assembly of the TCR heterodimer with the three dimeric signaling modules requires proper placement of a total of nine ionizable TM residues, the three basic TM residues of the TCR heterodimer (7, 19) and a pair of acidic TM residues in each signaling module (4). Each basic TCR TM residue serves a specific role in the assembly process; lysine residues located close to the center of the TM domains of TCRα and TCRβ serve as interaction sites for the CD3$\delta\varepsilon$ and CD3$\gamma\varepsilon$ dimers, respectively, whereas the arginine in the N-terminal third of the TCRα TM domain interacts with the $\zeta\zeta$ dimer (4). The formation of these three-chain TM interactions requires both acidic residues of each signaling module, because substitution of only one of these acidic residues greatly diminishes or abolishes complex formation (4, 20).

Several lines of evidence suggest contributions of the CD3 extracellular domains to assembly of TCR-CD3 complexes, but the location and precise nature of these interaction sites on CD3 dimers remain unknown. Global approaches have demonstrated physical proximity between TCR constant domains and CD3 dimers. Chemical cross-linking experiments demonstrated an interaction between TCRβ and CD3γ (21), a result consistent with the TM interaction of the acidic CD3$\gamma\varepsilon$ residues and the TCRβ lysine (4, 22). Furthermore, a mAb (H57) that binds to the TCR Cβ FG loop was shown to reduce subsequent staining with a CD3ε mAb (2C11) (23). Steric hindrance between these two mAbs does not provide fine resolution due to the fact that Fab fragments are similar in size to the entire TCR$\alpha\beta$ ectodomain.

TCR$\alpha\beta$-CD3 complexes contain only one copy of each CD3 dimer, despite the similarity of the lysine-based TM interaction sites for CD3$\delta\varepsilon$ and CD3$\gamma\varepsilon$ (4, 24, 25). At least two mechanisms contribute to the specific requirement for both CD3 dimers; the TCRα chain has a strong preference for interaction with CD3$\delta\varepsilon$, and efficient interaction of CD3$\gamma\varepsilon$ with TCRβ requires prior association of TCRα and CD3$\delta\varepsilon$ (4). A contribution of the CD3γ extracellular domains to specificity of assembly was shown by domain exchange; a CD3γ mutant with the TM domain of CD3δ was incorporated into full TCR-CD3 complexes, but a CD3γ mutant with the extracellular domain of CD3δ failed to be incorporated (4, 22, 26).

The persisting uncertainties about the physical nature of TCR-CD3 extracellular domain interactions have resulted in a number of competing models (2). Early models emphasized lateral interactions between Ig domains of TCR and CD3 dimers. However, a more recent model suggested the possibility that the CD3 ectodomains may be located close to the cell membrane underneath the TCR constant domains (27). This model is based on three facts: 1) the TM domains of TCRα-CD3$\delta\varepsilon$ and TCRβ-CD3$\gamma\varepsilon$ are within close proximity (4); 2) the CD3 stalks are substantially shorter than the TCR connecting peptides (2); 3) the location of

conserved glycans in CD3γ, CD3δ, and TCR$\alpha\beta$ excludes particular surfaces as candidates for such interactions (27). This model suggests that the stalk regions of TCRα-CD3$\delta\varepsilon$ and TCRβ-CD3$\gamma\varepsilon$ may form a three-chain interface. We therefore investigated whether the conserved C*XX*-C*X*E*XXX* motif present in all CD3 chains contributes to assembly of TCR-CD3 complexes.

EXPERIMENTAL PROCEDURES

Antibodies and Reagents

Anti-CD3ε (mouse mAb UCHT1) was obtained from Santa Cruz Biotechnology, Inc. (Santa Cruz, CA), and high affinity anti-hemagglutinin (anti-HA, rat mAb 3F10) and calcium-dependent anti-Protein C (anti-PC, mouse mAb HPC4) were from Roche Applied Science. Streptavidin coupled to agarose beads was purchased from Sigma, and digitonin was from Biosynth International (Naperville, IL).

cDNA Constructs and in Vitro Transcription

Human CD3γ, -δ, -ε, and -ζ constructs were generated form peripheral blood lymphocytes by reverse transcription-PCR, whereas TCRα and -β sequences originated from the A6 T cell clone (28). All sequences were cloned into a modified pSP64 vector (provided by M. Kozak) with the murine H-2K^b signal sequence (4). Mutations were introduced by PCR using overlapping primers. Peptide tags were added as C-terminal in-frame fusions, usually with a three-amino acid flexible linker. The streptavidin-binding peptide (SBP) was sequence C4 (29), with 4 methionines and 1 cysteine changed to serine so that radiolabeled methionine or cysteine would not be incorporated into the tag. Peptide tag sequences (single-letter code) were as follows: SBP (SDEKTTGWRGGHVVEGLAGELEQLRAR-LEHHPQGQREPSSSGGSKLG), PC (EDQVDPRLIDGK), and HA peptide (YPYDVPDYA). *In vitro* transcription was performed from linearized cDNA constructs using a RiboMax T7 large scale RNA production kit and methyl-^{7}G cap analog (Pro-mega, Madison, WI).

Translation and Assembly Reactions

Each 25-μl reaction contained 17.5 μl of nuclease-treated rabbit reticulocyte lysate (Promega), 0.5 μl of amino acid mixture minus cysteine and methionine (Promega), 0.5 μl of SUPERase-In RNase inhibitor (Ambion), 1.0 μl of ^{35}S-labeled methionine (Amersham Biosciences), equivalent molar amounts of each RNA (60–200 ng of each), and 2.0 μl of ER microsomes. These microsomes were prepared on continuous iodixanol gradients from a mouse IVD12 hybridoma (ATCC) as previously described (4). All translation and assembly reactions were performed at 30 °C. An initial translation period of 30 min under reducing conditions was followed by a 2–4-h assembly period (4 h for complete TCR-CD3 complexes, 2 h for any assembly intermediate) after the addition of GSSG to 4 mM. Reaction volumes were 25–100 μl as required for optimal signal with multistep sequential non-denaturing IP (snIP) procedures.

Immunoprecipitation, Electrophoretic Analysis, and Densitometry

Translation and assembly reactions were stopped by dilution with 1 ml of ice-cold TBS, 10 mM iodoacetamide, and microsomes were pelleted (10 min/20,800 g/4 °C) and rinsed. Pellets were resuspended in 20 μl of solubilization/IP buffer (TBS plus 0.5% digitonin, 10 mM iodoacetamide, 0.1% bovine serum albumin, 5 μg/ml leupeptin, 1 mM phenylmethylsulfonyl fluoride; with 1 mM $CaCl_2$ when anti-Protein C mAb was used) by vigorous pipetting and then rotated for 30 min at 4 °C in a total of 400 μl of solubilization/IP buffer. Lysates were pre-cleared for 1 h with PBS/bovine serum albumin-blocked Sepharose 4 beads, and primary captures were performed overnight at 4 °C. Primary IP products were washed twice in 0.5 ml of wash buffer (TBS plus 0.5% digitonin, 10 mM iodoacetamide; with 1 mM $CaCl_2$ for anti-Protein C mAb binding). Nondenaturing elution of SA-captured complexes was performed by incubation with 400 μl of solubilization/IP buffer with 100 μM free biotin for 1 h at 4 °C, and eluted complexes were incubated with subsequent antibodies and Protein G-Sepharose 4 beads (Amersham Biosciences) for 2 h at 4 °C and washed as before. Nondenaturing elution with EDTA (PC tag) was performed as described (4). Final precipitates were digested for 1 h at 37 °C with 500 units of endoglycosidase H (New England Biolabs), separated on 12% BisTris gels under nonreducing conditions (Invitrogen), transferred to polyvinylidene difluoride membranes, and exposed to PhosphorImager plates. Densitometry was performed using the Wide Line tool in the ImageQuant software package (Amersham Biosciences).

Chelation of Cations during TCR-CD3 Assembly

RNAs were translated for 30 min under reducing conditions to permit insertion of newly synthesized radiolabeled proteins into ER microsomes. 20 mM EDTA was then added to the reaction to chelate all divalent cations (0.5 mM Mg^{2+} is present in rabbit reticulocyte lysate); the same volume of water was added to control reactions. 4 mM GSSG was added simultaneously to initiate formation of structural disulfide bonds. Following a 2–4-h assembly period, membrane microsomes were pelleted and solubilized in IP buffer supplemented with 20 mM EDTA. TCR-CD3 complexes were isolated by one-step IP using the CD3ε-specific UCHT1 mAb. Endoglycosidase H digestion, electrophoresis, and densitometry were performed as described above.

RESULTS

The Membrane-proximal Tetracysteine Motif of CD3γε and CD3δε

The membrane-proximal segments of CD3γ, -δ, and -ε carry a highly conserved C*XX*C*X*E*XXX* sequence motif, and the two cysteines within this motif are located at positions −6 and −9 relative to the predicted TM segments (Fig. 1*A*). The NMR and crystal structures of CD3γε and CD3δε demonstrated that the G strands of the two chains form a long β-sheet at the dimer interface (27, 30, 31), as illustrated in Fig. 1*B* for human CD3γε and CD3δε. The cysteines were not included in these recombinant soluble proteins or could not be resolved in these structures, but the available structural information indicates that the four cysteines are located within close proximity in the stalk region of both CD3 dimers. Conserved arginines are located close to the C terminus of the β-strands, and the stalk starts with the first cysteine of this motif (Fig. 1*C*). The four cysteines may form two intrachain

disulfide bonds that stabilize the secondary structure of the CD3 stalk regions or may coordinate a divalent cation, such as zinc. The CD3 constructs that were used to probe the contribution of these cysteine residues to assembly of CD3 dimers with TCR are illustrated in Fig. 1*D*.

The Four Membrane-proximal Cysteine Residues Are Not Required for CD3δε or CD3γε Dimerization

We examined the assembly of CD3 dimers and their interaction with TCR using an *in vitro* translation system with ER microsomes isolated from a murine B cell hybridoma, and we and others have previously shown that this system faithfully reproduces protein interactions in the ER identified with metabolic labeling techniques in cells (4, 32, 33). Major advantages of this system are that a series of mutations can be evaluated in parallel under identical reaction conditions and that quantification of ^{35}S-labeled protein complexes provides highly reproducible measurements (25).

Previous studies based on Western blotting techniques had suggested that the membrane-proximal cysteines may contribute to formation of CD3 dimers (31, 34), and we therefore tested the efficiency of CD3 dimerization for mutants in which both membrane-proximal cysteines of CD3γ, -δ, and/or -ε were substituted by alanine (Fig. 2). CD3 complexes were isolated with the UCHT1 mAb that binds to an exposed surface epitope of CD3ε. This mAb is suitable for this analysis, because it immunoprecipitates properly folded CD3$\gamma\varepsilon$ and CD3$\delta\varepsilon$ dimers (Fig. 2, *lanes 1* and *2*), including CD3 dimers incorporated into TCR-CD3 complexes (Figs. 3–6) (4, 27, 35, 36). Ala-nine substitution of the two membrane-proximal cysteines of CD3ε (ε_{2CA}) did not reduce recovery of dimers with WT CD3γ or CD3δ (*lanes 4* and *5*). A mixing control (*, *lane 3*) in which the three chains were translated separately and then combined prior to solubilization of membranes with digitonin and IP demonstrated that dimer formation occurred in ER micro-somes and not following solubilization. Similar mutations of both cysteines in either CD3γ or CD3δ (γ_{2CA} and δ_{2CA}, respectively, *lanes 6* and *7*) did not impair dimer formation with WT CD3ε, and even alanine substitution of all four membrane-proximal cysteines did not reduce either CD3$\gamma\varepsilon$ or CD3$\delta\varepsilon$ dimerization (*lanes 8* and *9*).

Mutation of Membrane-proximal Cysteines Substantially Impairs Assembly of CD3δε with TCRα

The first major step in the assembly of TCR-CD3 complexes is the interaction of TCRα with the CD3$\delta\varepsilon$ dimer (4, 20), and we examined if mutation of the membrane-proximal cysteines of CD3δ or -ε affects this assembly step (Fig. 3). Three-chain complexes were isolated by two-step snIP using the calcium-dependent PC epitope tag attached to TCRα in the first IP step. Following elution with EDTA, complexes containing CD3ε were then isolated in the second IP step with the UCHT1 mAb. Substitution of the two cysteines at positions 72 and 75 of CD3δ substantially reduced assembly of CD3$\delta\varepsilon$ with TCRα (24% relative to WT; *lane 5*), and simultaneous substitution of all four membrane-proximal cysteines of the CD3$\delta\varepsilon$ dimer resulted in an almost complete assembly defect (5% relative to WT; *lane 7*). Substitution of the two cysteines in only CD3ε had only a subtle effect (*lane 3*), but these two cysteines contributed to assembly, because simultaneous mutation of CD3δ and CD3ε

resulted in a substantially more severe assembly defect than mutation of CD3δ alone (5% *versus* 24% relative to WT, respectively). Mixing controls (*, *lanes 2*, *4*, *6*, and *8*) demonstrated specificity of assembly, and parallel analysis of aliquots of reactions without IP (*lower panel*) confirmed the presence of equal quantities of input proteins.

Based on these results, we generated mutants in which the cysteines were individually substituted by alanine (δ_{C72A} and δ_{C75A}) and examined CD3$\delta\varepsilon$ dimerization as well as assembly with TCRα (Fig. 3*B*). Both point mutations reduced assembly with TCRα to a similar extent as simultaneous substitution of both cysteines (23–30% relative to WT; *lanes 8* and *9*). Loss of either one or both cysteine side chains may prevent formation of an intrachain disulfide bond and thus modify the conformation of the stalk region. We also generated a CD3δ mutant in which both cysteines were substituted by serine (δ_{2CS}); this mutant maintained the polar character and size of the side chains at positions 72 and 75 but lacked the ability to form a disulfide bond at this site. This mutant showed the same assembly defect as the single or double alanine mutants (*lane 10*).

Analysis of CD3δ mutants in which only a single cysteine was modified also demonstrated that the four cysteines in the stalk region were within close proximity; mutation of either cysteine resulted in the formation of covalent dimers with CD3ε (indicated by the *dagger* in Fig. 3*B*, *lanes 3* and *4*). The IP strategy used for this experiment ensured isolation of CD3 heterodimers, because the streptavidin-binding peptide (SBP) tag attached to CD3ε was used in the first IP step (elution with biotin), and the HA tag on CD3δ was used in the second step.

A TCRα Mutant Lacking the Entire Ig Domain Assembles with CD3δε

These results suggested that interactions among the membrane-proximal segments may be involved in assembly of TCRα with CD3$\delta\varepsilon$. We examined the structural requirements on the TCRα side by generating a mutant that contained the entire connecting peptide but lacked both variable and constant Ig domains (α_{TM2}) (Fig. 4*A*). This mutant assembled with CD3$\delta\varepsilon$ (Fig. 4*B*, *lane 3*), indicating that interaction among TCR Ig domains and CD3$\delta\varepsilon$ was not required for this step. Densitometry measurements of input radiolabeled proteins (Fig. 4*B*, *lower panel*) demonstrated that similar molar quantities of WT TCRα and α_{TM2} proteins were present in these reactions (*lanes 1* and *3*, respectively). Another mutant in which the TCRα connecting peptide was shortened to six residues (α_{TM1}) also bound to CD3$\delta\varepsilon$, but the yield of this three-chain complex was reduced (*lane 2*, 30% relative to WT).

Both TCRα mutants showed a pattern comparable with WT TCRα when analyzed against the panel of CD3δ mutants in which the membrane-proximal cysteines were substituted by alanine or serine (Figs. 3*B* and 4*C*). For example, the double serine CD3δ mutant (δ_{2CS}) showed a severe assembly defect with both α_{TM1} and α_{TM2} proteins (7–10% relative to WT CD3δ), indicating that loss of the TCRα Ig domains had not resulted in a different type of interaction with CD3$\delta\varepsilon$ for these proteins.

Mutation of Membrane-proximal Cysteines Also Affects Association of CD3γε with TCR but Not Association of the ζζ Dimer

The CD3$\gamma\varepsilon$ dimer assembles efficiently with TCR$\alpha\beta$ only in the presence of the CD3$\delta\varepsilon$ dimer (4), indicating that association of CD3$\gamma\varepsilon$ usually occurs following formation of the TCR-CD3$\delta\varepsilon$ assembly intermediate. We therefore assessed the effect of mutation of the membrane-proximal cysteines in the CD3$\gamma\varepsilon$ dimer in the context of the six-chain CD3$\delta\varepsilon$-TCR$\alpha\beta$-CD3$\gamma\varepsilon$ assembly intermediate by targeting the CD3γ (PC tag) and CD3δ (HA tag) chains in a two-step snIP (Fig. 5A). We have previously shown that this IP method yields stoichiometric quantities of all three dimers (1:1:1) (25). Mutation of the two cysteines in either CD3γ or CD3ε (γ_{2CA} and ε_{2CA}) moderately reduced recovery of the six-chain complex (*lanes 3* and *5*), but substitution of all four cysteines resulted in a severe assembly defect (*lane 7*, 11% relative to WT). In this experiment, the CD3ε mutation affected the interaction of both CD3$\delta\varepsilon$ and CD3$\gamma\varepsilon$ with TCR, but the results in Fig. 3*A* had demonstrated that the CD3ε mutation had only a modest effect in the context of the CD3$\delta\varepsilon$ dimer as long as CD3δ was WT (71% of CD3$\delta\varepsilon$-TCRα complexes relative to WT CD3ε). The observed reduction in the yield of six-chain complexes was thus primarily due to mutation of the four cysteines in the CD3$\gamma\varepsilon$ dimer. The results for the CD3$\gamma\varepsilon$ dimer were thus similar to CD3$\delta\varepsilon$, because mutation of all four cysteines had a more substantial effect than mutation of cysteines in only one chain (Figs. 3*A* and 5*A*). Mutation of the membrane-proximal cysteines of CD3γ and -ε did not affect the last assembly step, the association of the $\zeta\zeta$ dimer (Fig. 5*B*), because the reduction in recovery of fully assembled complexes resembled the reduction of six-chain complexes, indicating that there was no additional negative effect on the last assembly step. In fact, the yield of complexes with the CD3γ and -ε cysteine mutations was higher in the presence of $\zeta\zeta$ (*lane 6*, 57% of complexes relative to WT CD3γ and -ε) than in its absence (*lane 3*, 15% of complexes relative to WT), suggesting that the $\zeta\zeta$ dimer may stabilize complexes that incorporate these mutated CD3 chains.

Chelation of Divalent Cations Does Not Affect the Efficiency of TCR-CD3 Assembly

Clusters of cysteine residues can coordinate zinc or other cations (37), and we therefore examined the requirement for divalent cations during assembly of TCR-CD3 complexes as an alternative hypothesis to the formation of intrachain disulfide bonds described above. Once a divalent cation is buried at a protein-protein interface, dissociation may be very slow and occur only following dissociation of the complex. We therefore chose an experimental design in which divalent cations were chelated by EDTA prior to initiation of assembly. In the *in vitro* translation system, initial translation occurs under reducing conditions, and the reaction is shifted to mildly oxidizing conditions following insertion of radiolabeled proteins into ER microsomes to enable formation of structural disulfide bonds. All dimers that assemble into TCR-CD3 complexes require formation of structural disulfide bonds, and assembly thus does not occur under the reducing conditions of the initial translation period. A control experiment (Fig. 6*A*) confirmed that no CD3 dimers were formed during the initial translation period (*lanes 1* and *2*) and that the presence of EDTA had little effect on the subsequent formation of CD3 dimers (*lanes 3* and *4*). We added a large molar excess of EDTA (20 mM) following completion of the translation period and assessed whether the presence of EDTA during assembly would reduce the yield of TCRα-CD3$\delta\varepsilon$ three-chain

complexes (Fig. 6*B*) or full TCR-CD3 complexes (Fig. 6*C*). The results clearly demonstrated that chelation of divalent cations had no substantial effect on assembly, ruling out the possibility that the membrane-proximal tetracysteine motifs bind a divalent cation essential for interaction of CD3 dimers with TCR. A small reduction in recovery of the assembled complex was observed, most likely due to the fact that the presence of divalent cations promotes oxidative disulfide bond formation.

DISCUSSION

These results demonstrate that the tetracysteine motif in the membrane-proximal stalk regions of CD3$\gamma\varepsilon$ and CD3$\delta\varepsilon$ dimers is an important structural element for their assembly with TCR. Assembly was severely impaired (to ~10% or less compared with WT) when all four cysteines of a given CD3 dimer were mutated to alanine. The interaction of CD3$\delta\varepsilon$ with TCRα was examined in detail, and mutation of the two membrane-proximal cysteines of CD3δ to alanine or serine was found to substantially reduce assembly (to 23–30%). Mutation of the two cysteines of CD3ε only moderately affected interaction with TCRα, but simultaneous mutation of CD3δ and CD3ε resulted in an assembly defect (reduction to ~5%) considerably more severe than for the CD3δ mutant alone. Similarly, mutation of the two membrane-proximal cysteines of CD3γ moderately reduced assembly with TCR (to 46%), but combined CD3γ and CD3ε mutations again resulted in a severe assembly defect (to 11%). In this experiment, the CD3ε mutant was incorporated into both CD3$\gamma\varepsilon$ and CD3$\delta\varepsilon$ dimers, but it appeared that the assembly defect was primarily localized to the CD3$\gamma\varepsilon$ side, because the CD3ε mutation alone only moderately affected the CD3$\delta\varepsilon$-TCRα interaction. These are the first point mutations in the CD3 extracellular domains shown to significantly impact assembly of CD3 dimers with TCR.

Previous studies had suggested that the C*XX*C motifs contribute to CD3 dimer formation. Borroto *et al.* (34) transfected COS cells with human CD3 constructs in which the cysteines in the C*XX*C motif of CD3ε were mutated to alanine. CD3ε chains were immunoprecipitated with the APA1/1 mAb and associated CD3γ or CD3δ were visualized by Western blotting (34). Sun *et al.* (31) also transfected COS cells but performed immunoprecipitation and Western blot analysis with antibodies to attached HA and FLAG epitope tags. These authors mutated the cysteines of murine CD3ε to serine but did not observe a substantial reduction in the efficiency of assembly with CD3γ (67% of WT), in contrast to the results reported by Borroto *et al.* (34) with a CD3ε alanine mutant. However, introduction of three additional mutations (at Tyr^{59}, Tyr^{72}, and Tyr^{74}) located N-terminal to Cys^{80} and Cys^{83} of CD3ε severely impaired CD3$\gamma\varepsilon$ dimer formation (31). We performed a comprehensive analysis in which the C*XX*C motif was mutated in all three CD3 chains and found that even mutation of all four membrane-proximal cysteines did not reduce CD3$\gamma\varepsilon$ or CD3$\delta\varepsilon$ dimer formation. The cysteine residues thus do not appear to be required for CD3 dimerization, unless the dimer interface is weakened by introduction of several other mutations. This conclusion is consistent with the finding that CD3$\gamma\varepsilon$ and CD3$\delta\varepsilon$ can be refolded from proteins expressed in *Escherichia coli* that lack the C*XX*C motifs (30, 31).

Our mutagenesis experiments also demonstrate that the cysteines can form covalent CD3$\delta\varepsilon$ dimers when a single cysteine in the C*XX*C motif is mutated to alanine (Fig. 3*B*). The

cysteines of CD3δ and CD3ε chains are thus within sufficient proximity to form an interchain disulfide bond, and the absence of such interchain disulfide bonds in properly folded CD3$\gamma\varepsilon$ and CD3$\delta\varepsilon$ dimers indicates that the SH groups are either stably bound to an unknown polar ligand or that they have already formed stable intrachain disulfide bonds prior to CD3 dimerization.

We considered the possibility that the tetracysteine motif may coordinate a cation such as zinc. Cysteine-based motifs coordinate zinc and other cations in many different proteins, such as the DNA binding domain of the glucocorticoid receptor. The glucocorticoid receptor DNA binding domain has two zinc-containing regions, and each binds zinc through four cysteine residues. The first zinc binding site is formed by two C*XX*C motifs, and the bound zinc ion stabilizes the α-helix that binds in the major groove of double-stranded DNA (37, 38). However, assembly of the CD3$\delta\varepsilon$-TCRα intermediate or complete TCR-CD3 complexes was not reduced when cations were chelated with EDTA. The mutagenesis experiments also argue against an essential role of a coordinated cation in assembly of CD3 dimers with TCR. Mutation of the two cysteines in one chain of a CD3 dimer would be predicted to destroy a metal coordination site, yet mutation of the C*XX*C motif in CD3ε alone only modestly reduced assembly of CD3$\delta\varepsilon$ with TCRα.

An alternative explanation for the important structural role of the C*XX*C motifs is that the two membrane-proximal cysteines of a given CD3 chain form an intrachain disulfide bond, as previously suggested by Borroto *et al.* (34). Several lines of evidence support this hypothesis. The close physical proximity of the two cysteines may favor rapid formation of intrachain disulfide bonds upon insertion of the nascent protein chain into the oxidizing environment of the ER, and formation of these disulfide bonds may occur more rapidly than folding of the Ig domain and subsequent CD3 dimerization. Rapid formation of an intrachain disulfide bond may thus explain why properly folded CD3$\gamma\varepsilon$ or CD3$\delta\varepsilon$ dimers lack interchain disulfide bonds. C*XX*C motifs form the catalytic site of thioredoxin and related enzymes, and the two cysteines form a disulfide bond at a particular step in the catalytic cycle, indicating that cysteines in C*XX*C motifs can be within sufficient proximity for disulfide bond formation. The N-terminal cysteine in the C*XX*C motif of thioredoxin serves as a nucleophilic attacking group and forms a transient disulfide bond with the substrate protein. Subsequent attack of this disulfide by the C-terminal cysteine releases the reduced product and results in the formation of a disulfide bond between the two cysteines of the C*XX*C motif (39, 40).

We made substantial efforts to isolate the membrane-proximal domains for analysis by mass spectrometry to directly demonstrate the presence of intrachain disulfide bonds (the presence of the disulfide bond is predicted to reduce the molecular mass of the peptide by 2 daltons). However, despite the use of multiple enzymes and isolation techniques, membrane-proximal or TM domain cleavage fragments could not be identified by mass spectrometry, although many other fragments were identified at high redundancy. Proteolytic cleavage of the membrane-proximal fragment may be impaired by the neighboring TM domain, and recovery of long fragments containing the TM may be reduced by their hydrophobicity and/or bound detergent. Nevertheless, all available data are consistent with the hypothesis

that the four membrane-proximal cysteines serve a structural role by forming two intrachain disulfide bonds in the CD3 stalk regions.

Much effort in the field has focused on identifying contacts between the Ig domains of CD3 dimers and TCR (2), but point mutations that substantially impair assembly had not been identified. This study demonstrates that the stalk regions of the CD3 dimers are important structural elements for the interaction of CD3 dimers with TCR. This conclusion is also supported by the finding that a TCRα mutant containing the entire connecting peptide but lacking the Ig domains assembled with CD3$\delta\varepsilon$, whereas a mutant in which the connecting peptide was shortened to six residues assembled at a reduced level. A structural role of the CD3 stalk region C*XX*C motifs in assembly is also consistent with the reported finding that mutations in the TCRα connecting peptide impair TCR signaling (41). The membrane-proximal C*XX*C motifs may contribute to the secondary structure of the CD3 stalk regions and may also help to properly position the CD3 TM domains for interaction with the appropriate TCR TM helix.

References

1. Oettgen HC, Terhorst C. Crit Rev Immunol. 1987; 7:131–167. [PubMed: 2953555]
2. Kuhns MS, Davis MM, Garcia KC. Immunity. 2006; 24:133–139. [PubMed: 16473826]
3. Samelson LE, Harford JB, Klausner RD. Cell. 1985; 43:223–231. [PubMed: 3878228]
4. Call ME, Pyrdol J, Wiedmann M, Wucherpfennig KW. Cell. 2002; 111:967–979. [PubMed: 12507424]
5. Punt JA, Roberts JL, Kearse KP, Singer A. J Exp Med. 1994; 180:587–593. [PubMed: 8046335]
6. Ashwell JD, Klausner RD. Annu Rev Immunol. 1990; 8:139–167. [PubMed: 2188661]
7. Blumberg RS, Alarcon B, Sancho J, McDermott FV, Lopez P, Breitmeyer J, Terhorst C. J Biol Chem. 1990; 265:14036–14043. [PubMed: 2143190]
8. Blumberg RS, Ley S, Sancho J, Lonberg N, Lacy E, McDermott F, Schad V, Greenstein JL, Terhorst C. Proc Natl Acad Sci U S A. 1990; 87:7220–7224. [PubMed: 2144901]
9. de la Hera A, Muller U, Olsson C, Isaaz S, Tunnacliffe A. J Exp Med. 1991; 173:7–17. [PubMed: 1824636]
10. Exley M, Terhorst C, Wileman T. Semin Immunol. 1991; 3:283–297. [PubMed: 1686832]
11. Weissman AM, Frank SJ, Orloff DG, Mercep M, Ashwell JD, Klausner RD. EMBO J. 1989; 8:3651–3656. [PubMed: 2583115]
12. Sussman JJ, Bonifacino JS, Lippincott-Schwartz J, Weissman AM, Saito T, Klausner RD, Ashwell JD. Cell. 1988; 52:85–95. [PubMed: 3278811]
13. Weissman AM, Baniyash M, Hou D, Samelson LE, Burgess WH, Klausner RD. Science. 1988; 239:1018–1021. [PubMed: 3278377]
14. Krissansen GW, Owen MJ, Fink PJ, Crumpton MJ. J Immunol. 1987; 138:3513–3518. [PubMed: 2952720]
15. Krissansen GW, Owen MJ, Verbi W, Crumpton MJ. EMBO J. 1986; 5:1799–1808. [PubMed: 2944745]
16. van den Elsen P, Shepley BA, Borst J, Coligan JE, Markham AF, Orkin S, Terhorst C. Nature. 1984; 312:413–418. [PubMed: 6095101]
17. Gold DP, Puck JM, Pettey CL, Cho M, Coligan J, Woody JN, Terhorst C. Nature. 1986; 321:431–434. [PubMed: 3012357]
18. Gold DP, Clevers H, Alarcon B, Dunlap S, Novotny J, Williams AF, Terhorst C. Proc Natl Acad Sci U S A. 1987; 84:7649–7653. [PubMed: 3478717]
19. Alcover A, Mariuzza RA, Ermonval M, Acuto O. J Biol Chem. 1990; 265:4131–4135. [PubMed: 2137462]

20. Kearse KP, Roberts JL, Singer A. Immunity. 1995; 2:391–399. [PubMed: 7719941]
21. Brenner MB, Trowbridge IS, Strominger JL. Cell. 1985; 40:183–190. [PubMed: 3871355]
22. Dietrich J, Neisig A, Hou X, Wegener AM, Gajhede M, Geisler C. J Cell Biol. 1996; 132:299–310. [PubMed: 8636209]
23. Ghendler Y, Smolyar A, Chang HC, Reinherz EL. J Exp Med. 1998; 187:1529–1536. [PubMed: 9565644]
24. Geisler C. J Immunol. 1992; 148:2437–2445. [PubMed: 1532815]
25. Call ME, Pyrdol J, Wucherpfennig KW. EMBO J. 2004; 23:2348–2357. [PubMed: 15152191]
26. Wegener AM, Hou X, Dietrich J, Geisler C. J Biol Chem. 1995; 270:4675–4680. [PubMed: 7533164]
27. Arnett KL, Harrison SC, Wiley DC. Proc Natl Acad Sci U S A. 2004; 101:16268–16273. [PubMed: 15534202]
28. Garboczi DN, Ghosh P, Utz U, Fan QR, Biddison WE, Wiley DC. Nature. 1996; 384:134–141. [PubMed: 8906788]
29. Wilson DS, Keefe AD, Szostak JW. Proc Natl Acad Sci U S A. 2001; 98:3750–3755. [PubMed: 11274392]
30. Kjer-Nielsen L, Dunstone MA, Kostenko L, Ely LK, Beddoe T, Mifsud NA, Purcell AW, Brooks AG, McCluskey J, Rossjohn J. Proc Natl Acad Sci U S A. 2004; 101:7675–7680. [PubMed: 15136729]
31. Sun ZJ, Kim KS, Wagner G, Reinherz EL. Cell. 2001; 105:913–923. [PubMed: 11439187]
32. Huppa JB, Ploegh HL. J Exp Med. 1997; 186:393–403. [PubMed: 9236191]
33. Ribaudo RK, Margulies DH. J Immunol. 1992; 149:2935–2944. [PubMed: 1401922]
34. Borroto A, Mallabiabarrena A, Albar JP, Martinez AC, Alarcon B. J Biol Chem. 1998; 273:12807–12816. [PubMed: 9582308]
35. Burns GF, Boyd AW, Beverley PC. J Immunol. 1982; 129:1451–1457. [PubMed: 6980937]
36. Borst J, Prendiville MA, Terhorst C. Eur J Immunol. 1983; 13:576–580. [PubMed: 6223826]
37. Hard T, Kellenbach E, Boelens R, Maler BA, Dahlman K, Freedman LP, Carlstedt-Duke J, Yamamoto KR, Gustafsson JA, Kaptein R. Science. 1990; 249:157–160. [PubMed: 2115209]
38. Luisi BF, Xu WX, Otwinowski Z, Freedman LP, Yamamoto KR, Sigler PB. Nature. 1991; 352:497–505. [PubMed: 1865905]
39. Ritz D, Beckwith J. Annu Rev Microbiol. 2001; 55:21–48. [PubMed: 11544348]
40. Powis G, Montfort WR. Annu Rev Biophys Biomol Struct. 2001; 30:421–455. [PubMed: 11441809]
41. Backstrom BT, Milia E, Peter A, Jaureguiberry B, Baldari CT, Palmer E. Immunity. 1996; 5:437–447. [PubMed: 8934571]

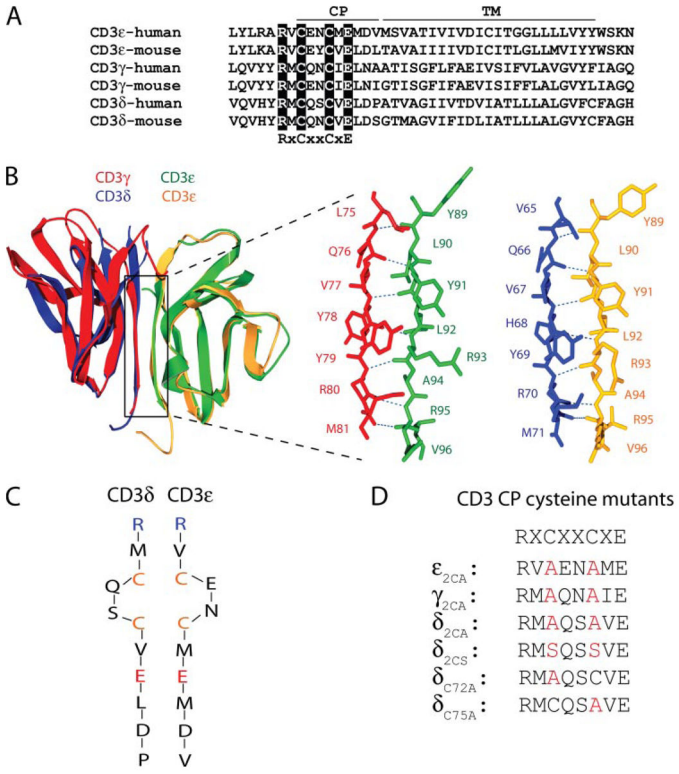

FIGURE 1. A highly conserved membrane-proximal tetracysteine motif in the stalk region of CD3*γε* and CD3*δε* dimers

A, sequence alignment of human and mouse CD3*γ*, -*δ*, and -*ε* sequences in the membrane-proximal extracellular and TM domains. The conserved C*XX*C*X*E*XXX* motif in the connecting peptide (*CP*) and the conserved arginine at the −2-position relative to this motif are *highlighted. B*, *ribbon diagrams* of the crystal structures of human CD3*γε* and CD3*δε* extracellular domains overlaid based on the *ε* chain present in both dimers (Protein Data Bank code 1SY6 and 1XIW, respectively) (27, 30). The parallel *β*-strands of each subunit that create a *β*-sheet at the dimer interface are *boxed* on the *left* and shown separately for CD3*γε* (*γ*, *red; ε*, *green*) and CD3*δε* (*δ*, *blue; ε*, *yellow*) on the *right. C*, the cysteines comprising the tetracysteine motif are located within close proximity of each other in the stalk region of CD3*δε* (and CD3*γε*). The membrane-proximal CD3*δ* and CD3*ε* sequences are aligned, starting with the conserved arginine residues at the C-terminal end of the *β*-strands shown in *B*. The cysteines do not form interchain disulfide bonds in assembly-competent CD3*δε* or CD3*γε* dimers. Rather, they may form intrachain disulfide bonds or coordinately bind a polar ligand. *D*, mutants used to probe the role of tetracysteine motifs in assembly of CD3 dimers with TCR.

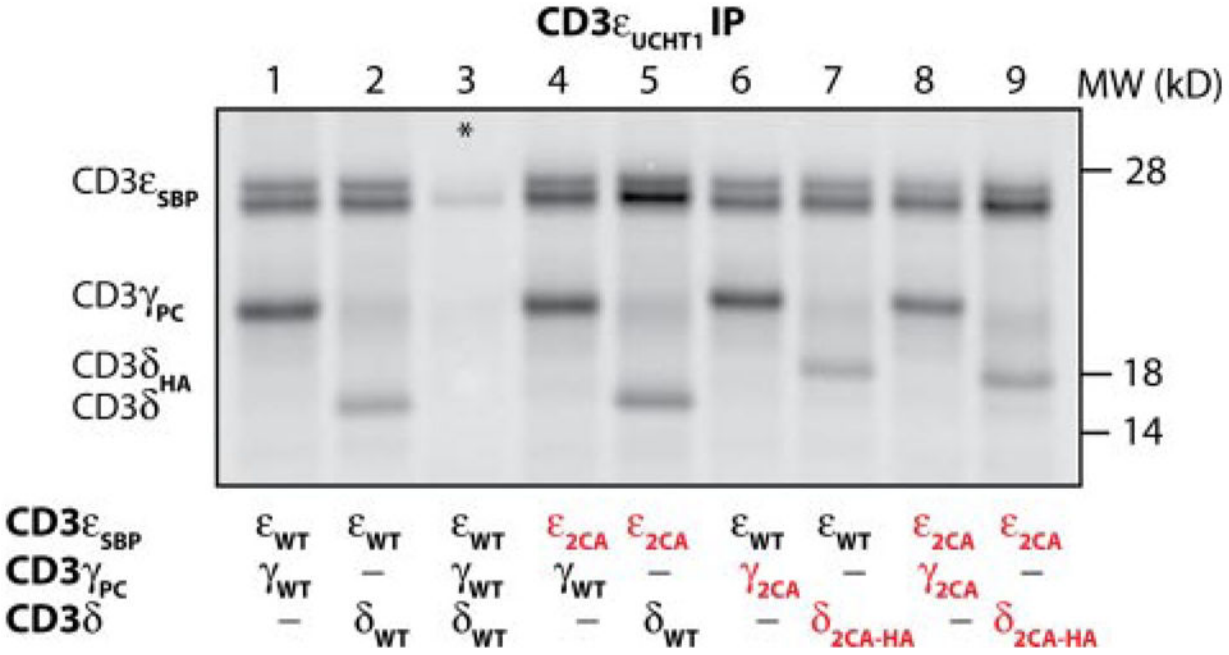

FIGURE 2. The membrane-proximal cysteine residues are not required for CD3 dimer formation

CD3*γε* and CD3*δε* dimer formation was examined using an *in vitro* translation system with ER microsomes using RNAs for CD3*γ*, CD3*δ*, and CD3*ε* WT constructs (*lanes 1* and *2*) or mutants in which both membrane-proximal cysteines of one chain (*lanes 4 –7*) or two chains (*lanes 8* and *9*) were substituted by alanine. The conformation-sensitive UCHT1 mAb specific for CD3*ε* was used in the IP. In a mixing control (*), CD3*γ*, -*δ*, and -*ε* RNAs were translated separately, and the contents of these reactions were combined prior to detergent solubilization and IP.

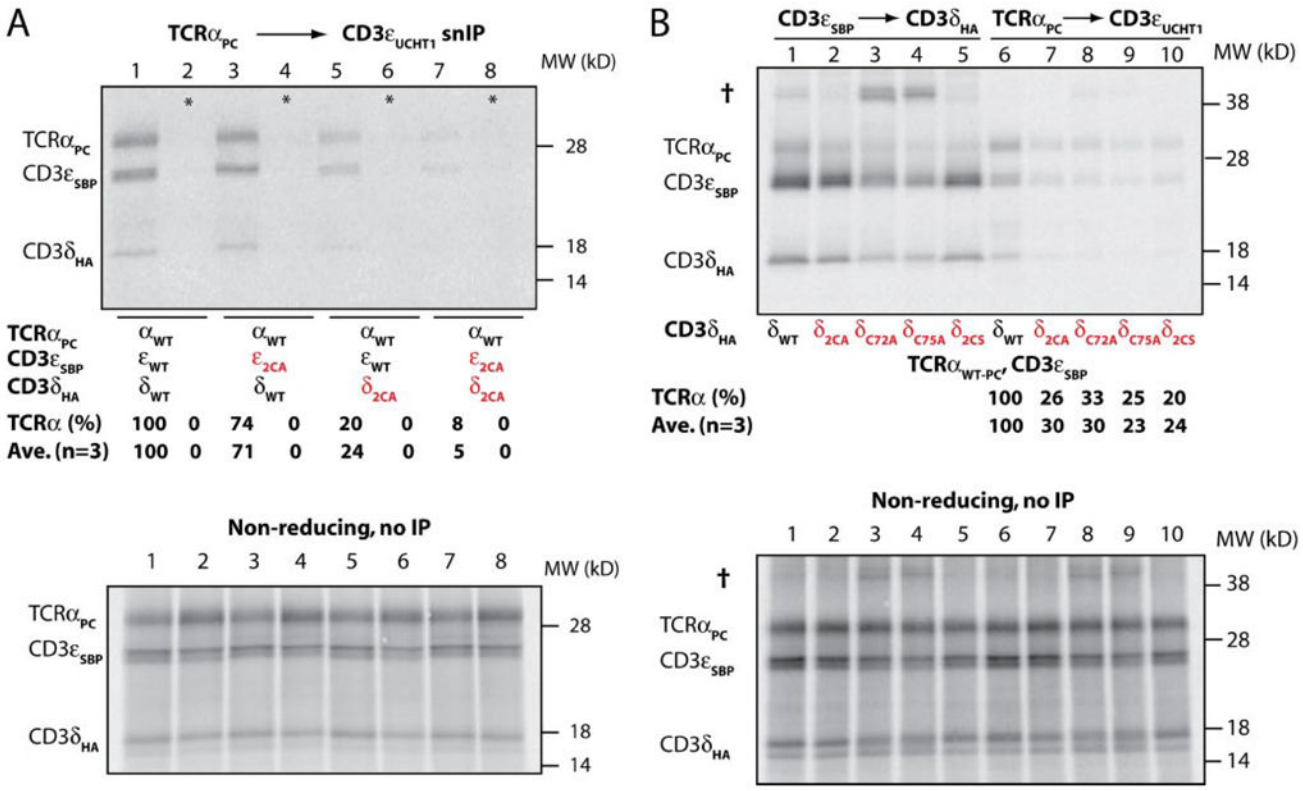

FIGURE 3. The membrane-proximal cysteines of CD3*δε* contribute to assembly with TCR*α*

A, CD3*ε* and CD3*δ* mutants in which both membrane-proximal cysteines were substituted by alanine (ε_{2CA} and δ_{2CA}, respectively) were analyzed for their ability to assemble into a three-chain TCR*α*-CD3*δε* complex. TCR*α*-CD3 complexes were isolated by two-step snIP using the PC tag attached to TCR*α* and the CD3*ε*-specific UCHT1 mAb. The amount of immunoprecipitated TCR*α* was quantitated relative to the reaction with WT sequences (*lane 1*). Substitution of the two membrane-proximal cysteines of CD3*δ* to alanine substantially reduced assembly with TCR*α* (*lane 5*), and substitution of all four membrane-proximal cysteines diminished assembly to less than 10% relative to WT (*lane 7*). *Lanes 2*, *4*, *6*, and *8* represent mixing controls (*) in which TCR*α* and CD3*δε* RNAs were translated in separate reactions that were combined prior to detergent solubilization of ER membranes. SDS-PAGE of aliquots of reactions prior to IP (*lower panel*) demonstrated equal quantities of input proteins. *B*, analysis of CD3*δ* mutants. CD3*δ* mutants were analyzed for their ability to form CD3*δε* dimers (*lanes 1–5*) and to assemble into TCR*α*-CD3*δε* complexes (*lanes 6 – 10*). The two membrane-proximal cysteines were either both substituted by alanine (δ_{2CA}, *lanes 2* and *7*) or serine (δ_{2CS}, *lanes 5* and *10*) or individually substituted by alanine (δ_{C72A} and δ_{C75A}, *lanes 3*, *4*, *8*, and *9*). CD3*δε* dimer formation was assessed by two-step snIP targeting the SBP tag on CD3*ε* and the HA tag on CD3*δ* (*lanes 1–5*), whereas TCR*α*-CD3*δε* complexes were isolated using the PC tag attached to TCR*α* and the CD3*ε* specific UCHT1 mAb (*lanes 6–10*). Even conservative substitution of the two CD3*δε* cysteines by serine substantially reduced assembly with TCR*α* (*lane 10*) but did not affect CD3*δε* dimerization (*lane 5*). Mutation of single membrane-proximal cysteines resulted in formation of covalent CD3*δε* dimers (†, *lanes 3* and *4*), indicating that the cysteines comprising the tetracysteine

motif are within close proximity. Analysis of aliquots of translation reactions prior to IP demonstrated equal quantities of input proteins (*lower panel*).

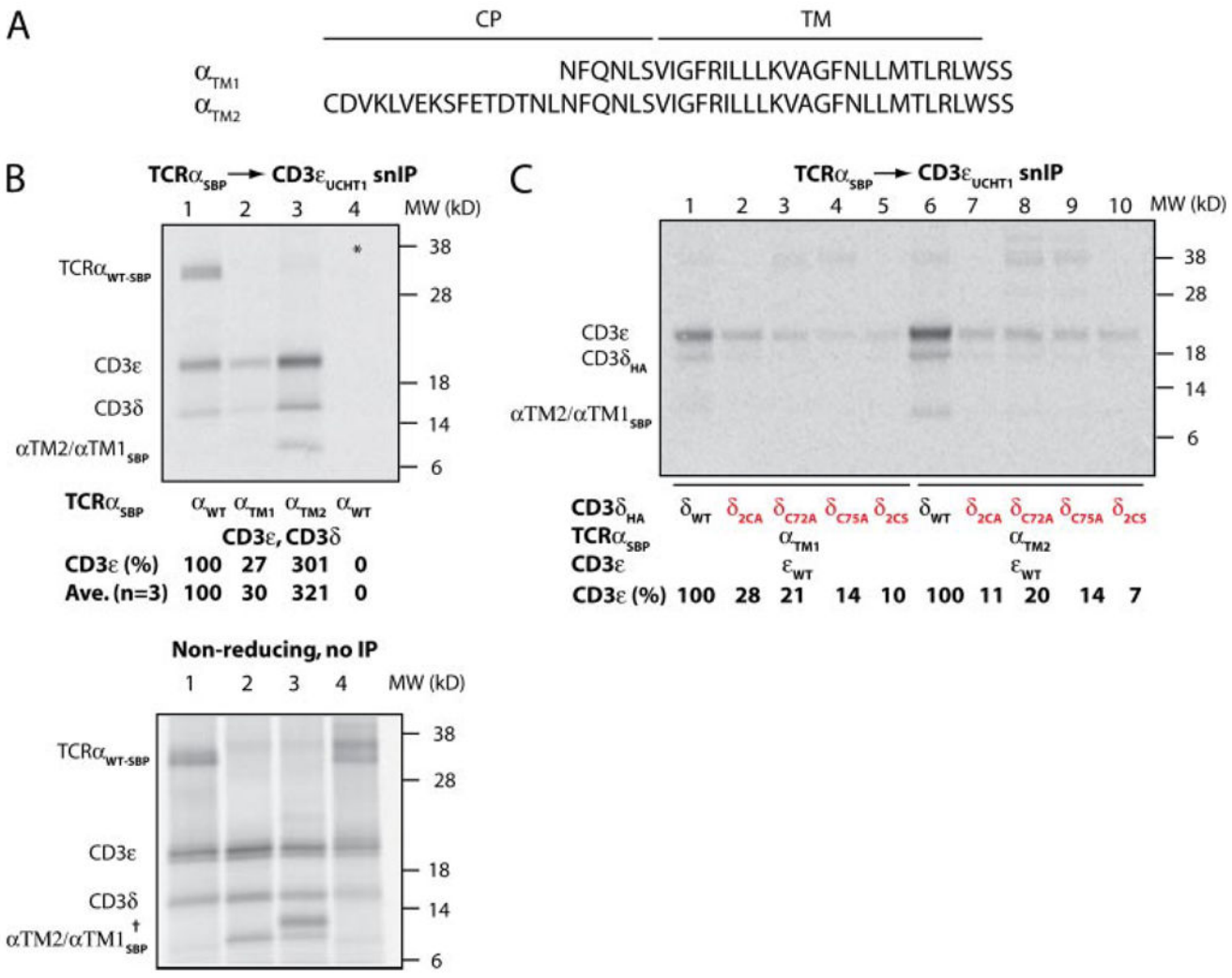

FIGURE 4. A TCR*α* mutant lacking both Ig domains assembles with CD3*δε*

A, TCR*α* assembly with the CD3*δε* dimer was compared for full-length TCR*α*, a mutant lacking the two TCR*α* Ig domains (α_{TM2}), and a mutant in which the connecting peptide was shortened to six residues (α_{TM1}). *B*, complexes containing these TCR*α* constructs and CD3*δε* were isolated by two-step snIP using the SBP tag on TCR*α* and the CD3*ε*-specific UCHT1 mAb. The α_{TM2} construct lacking both TCR*α* Ig domains assembled with CD3*δε*; assembly occurred at reduced levels with the shorter α_{TM1} construct. The α_{TM1} peptide was targeted in the first IP step and was therefore present in the isolated complex, but this short peptide was difficult to visualize at the quantities isolated in this IP (*lane 2*). Signal peptide cleavage of α_{TM2} protein was incomplete (†, *lane 3* of the *no IP* gel in the *lower panel*). The mixing control in *lane 4* (*) in which TCR*α* and CD3*δε* chains were translated separately and mixed prior to detergent solubilization demonstrated specificity of assembly. *C*, CD3*δ* cysteine mutants yield similar results with the TCR*α* mutants as with WT TCR*α*. Three-chain assembly reactions were set up with CD3*δ*, CD3*ε*, and SBP-tagged TCR α_{TM1} or α_{TM2} peptides, and three-chain complexes were isolated as in *B*. Substitution of one or both cysteine residues by alanine (δ_{C72A}, δ_{C75A}, and δ_{2CA}, respectively) or serine (δ_{2CS})

substantially reduced assembly of either TCR α_{TM1} or α_{TM2} with CD3$\delta\varepsilon$. The amount of immunoprecipitated CD3ε in reactions with these CD3δ mutants was compared with reactions with WT CD3δ.

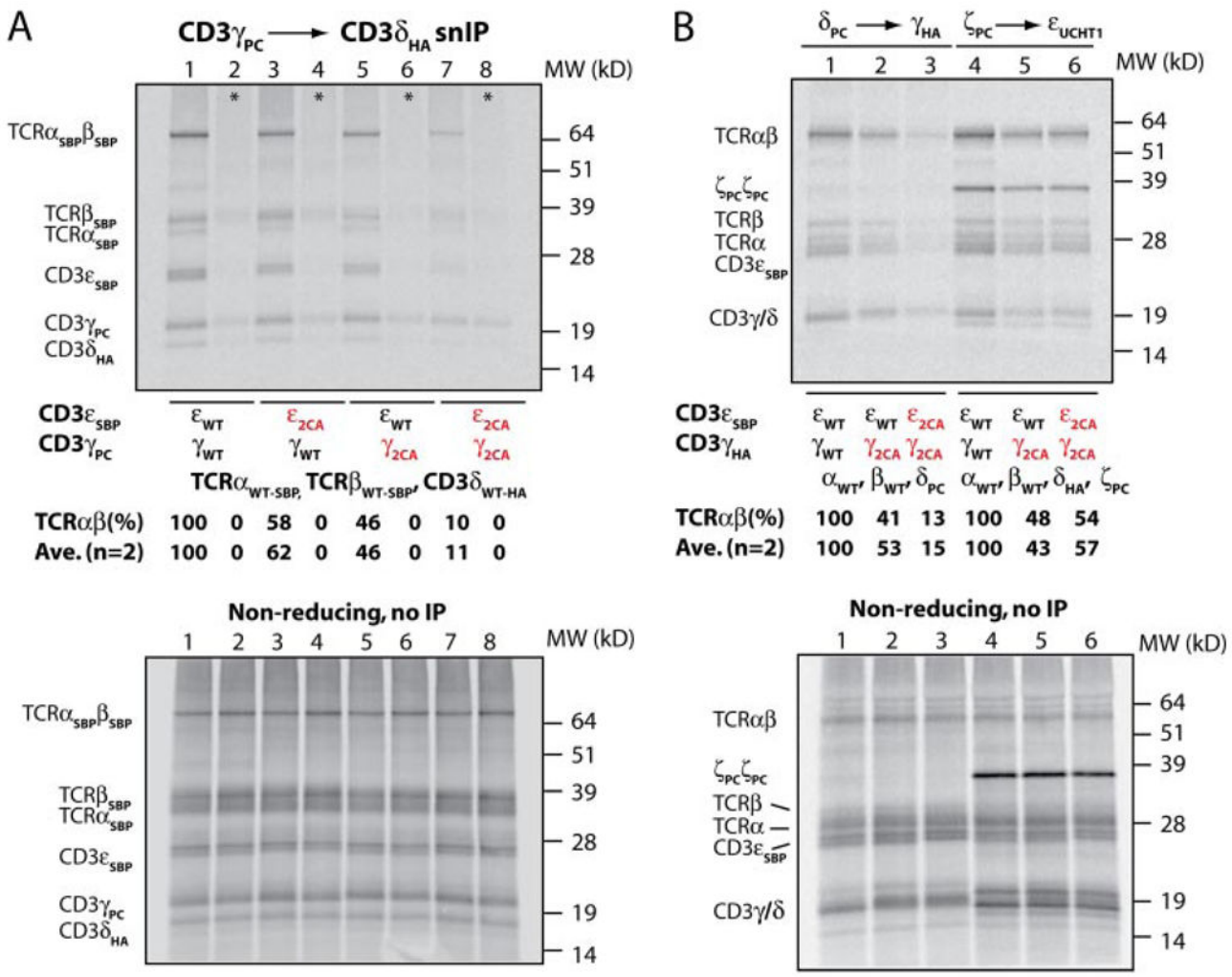

FIGURE 5. Role of tetracysteine motifs in formation of the six-chain CD3*δε*-TCR*αβ*-CD3*γε* intermediate

A, assembly of the six-chain complex was examined in reactions with TCR*α*, TCR*β*, and CD3*γ*, -*δ*, and -*ε*. TCR complexes containing both CD3*γε* and CD3*δε* were isolated by two-step snIP utilizing the PC and HA tags attached to CD3*γ* and CD3*δ*, respectively. The other components (TCR*α*, TCR*β*, and CD3*ε*) carried SBP tags to facilitate resolution of all components by SDS-PAGE. Substitution of the two membrane-proximal cysteines by alanine in only CD3*γ* (γ_{2CA}) or CD3*ε* (ε_{2CA}) moderately reduced assembly of the six-chain complex, but introduction of these mutations into both CD3*γ* and CD3*ε* chains (γ_{2CA} and ε_{2CA}) resulted in a severe assembly defect. *B*, the cysteine mutations do not affect the final assembly step, association of the *ζζ* dimer. Assembly reactions with all TCR-CD3 components (*lanes 4 – 6*) were compared with reactions lacking the *ζ* chain (*lanes 1–3*). Complete TCR-CD3 complexes were isolated by two-step snIP targeting the *ζ* chain (PC tag) and CD3*ε* (UCHT1 mAb) (*lanes 4 – 6*), whereas six-chain complexes were isolated from reactions lacking the *ζ* chain by two-step snIP targeting CD3*δ* (PC tag) and CD3*γ* (HA tag) (*lanes 1–3*).

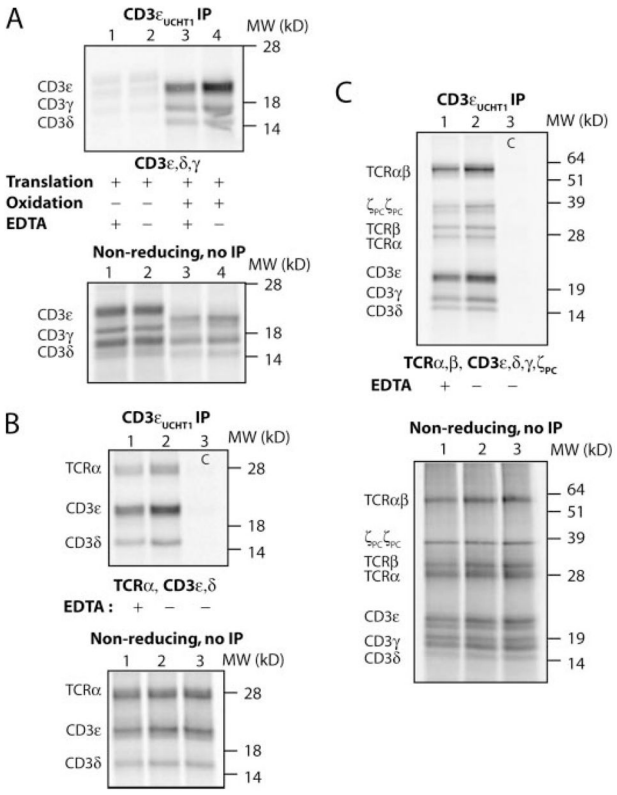

FIGURE 6. Chelation of divalent cations does not interfere with assembly of complete TCR-CD3 complexes

A, a control experiment confirmed that CD3 dimers do not form under the reducing conditions of the initial translation period. Following this translation period of 30 min, reactions in *lanes 3* and *4* were oxidized by the addition of oxidized glutathione. CD3 dimers were immunoprecipitated using the UCTH1 mAb after a 2-h assembly period. *B*, the addition of EDTA does not prevent assembly of TCR*α*with CD3*δε*. Three-chain complexes were isolated with the UCHT1 mAb even when EDTA was added before the 2-h assembly period. *Lane 3* represents an IP specificity control (*C*) with an isotype control antibody. *C*, the presence of EDTA does not interfere with formation of complete TCR-CD3 complexes. Specificity of IP was demonstrated by replacing the CD3*ε*-specific UCHT1 mAb (*lanes 1* and *2*) with an isotype control mAb (*lane 3*).